

The long-range detection of an accidental underwater explosion

Mark K Prior¹, Ross Chapman², Arthur Newhall³

¹International Data Centre, CTBTO Preparatory Commission, Vienna International Centre, Vienna, Austria, mark.prior@ctbto.org

²*School of Earth and Ocean Sciences, University of Victoria, BC, Canada, chapman@uvic.ca*

³*Woods Hole Oceanographic Institution, Massachusetts, USA, anewhall@whoi.edu*

During the Shallow Water 2006 Experiment, SW06, a power supply for seabed-moored oceanographic equipment suffered an accidental explosion. The equipment was located on the New Jersey Shelf, 175 kilometers south-east of New York. Acoustic signals emitted by the explosion were detected by hydrophone sensors that form part of the International Monitoring System (IMS) of the Comprehensive Test-Ban Treaty Organization (CTBTO). The IMS hydrophones were located at Ascension Island, approximately 8,000 kilometers away from the explosion site. The signals received on the IMS hydrophones are described and their arrival times and azimuths compared with theoretical values derived from underwater acoustic propagation modeling. It is shown that the differences between predicted and observed values of arrival time are less than 2 seconds, indicating an error in travel time prediction of 0.04%.

Measured azimuths are shown to be within 0.1 degrees of values derived on the assumption great circle propagation. While the explosion's location was theoretically visible from other IMS sensors, it was only detected on the sensors at Ascension Island. The reasons for the absence of any other detection are discussed. The views expressed are those of the authors and do not necessarily reflect the views of the CTBTO Preparatory Commission.

1 Introduction

The preparatory commission for the comprehensive nuclear-test-ban treaty organisation (CTBTO) operates the International Monitoring System (IMS), a global network of sensors which includes hydroacoustic stations designed to detect signals propagating through the ocean [dGH]. The hydroacoustic network uses two types of station – hydrophone and T-stations. Hydrophone stations use hydrophone triads deployed in the ocean deep-sound-channel while T-stations use seismometers located on land, near to the coast. Hydrophone triads are deployed in a two-kilometre-side, triangular configuration in the horizontal plane. This allows the arrival azimuth of signals to be determined from measurements of the time differences between signal arrivals at the three hydrophones. The hydrophones are placed at a depth designed to put them at the local axis of the deep sound channel [Urlick]. Hydrophone signals are sampled at 250 Hz but the roll-off of the anti-aliasing filter used restricts the effective upper frequency to around 100Hz.

As part of the IMS hydroacoustic network, hydrophone triads are located to the north and south of Ascension Island in the Atlantic Ocean. These are named H10N and H10S respectively and Fig. 1 shows the location of the northern site and the shore station from which power and signal cabling is run to the triads. On the third of August 2006, hydrophones at both the north and south triads received signals from a small explosion that took place on the New Jersey shelf (Fig. 2) as a result of a gas leak in the lithium battery pack of a seabed-moored current profiler. The path between explosion site and receiver location is shown in Fig. 3.

Arrival times and azimuths of signals detected on stations in the IMS hydroacoustic network are used as inputs to automatic processing routines [Hanson et al] that combine them with similar information measured at other stations to

hypothesize the times and locations of the events that generated the signals. This association is not restricted to signals from the hydroacoustic network and signals recorded on IMS seismic and infrasound networks [CTBT] can be associated with hydroacoustic signals and fused to produce event solutions. Correct signal association and accurate event location require both accurate measurement of arrival properties and reliable travel-time tables. Furthermore, a relationship must be assumed between the arrival azimuth and the path travelled through the ocean. For hydroacoustic signals, travel-time tables are generated by full-wave propagation model calculations using inputs from global environmental databases [UAM2009]. Horizontal ray paths are calculated ignoring the effects of lateral refraction or out-of-plane reflection from seabed slopes. Assessment of the accuracy of this approach is important to studies that attempt to quantify the quality of CTBTO's event solutions. The signals from the explosion on the New Jersey Shelf represented a "source of opportunity" that allowed this accuracy to be measured for one specific case.

The signals received on the hydrophones as a result of the explosion are described in the following section. In section 3, the observed arrival times and azimuths of the signal are compared with predicted values derived using "ground truth" information of the explosion's time and location. The reasons why the signal was not observed at the two other IMS hydroacoustic stations to which there existed possible paths are discussed in section 4. The significance of the differences between observed and ground truth arrival times and azimuths is then discussed.



Fig 1. Ascension Island with IMS hydroacoustic stations marked. White line shows direction of explosion site. Southern hydrophone triad is 110 km SSW

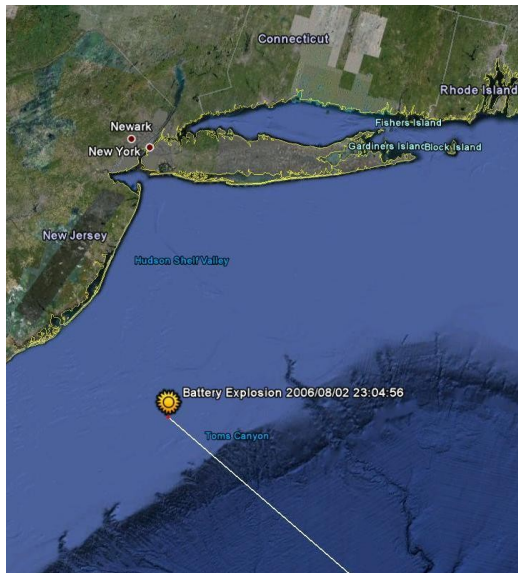


Fig 2. New Jersey Shelf region, showing explosion site. White line indicates direction to Ascension Island.

2 Signal characteristics

The signals recorded on the northern triad are shown in Fig. 4 in the form of a spectrogram and time series. The time series show a crescendo form with intensity rising at an increasing rate until the signal is terminated by a sharp cut-off. This form is typical of signals that have propagated through the deep sound channel [Urlick]. The spectrogram in Fig. 4 shows the dispersive nature of propagation with the lowest frequency content of the signal, between 5 Hz and 10Hz, terminating a few seconds before the higher frequencies of up to 80 Hz.

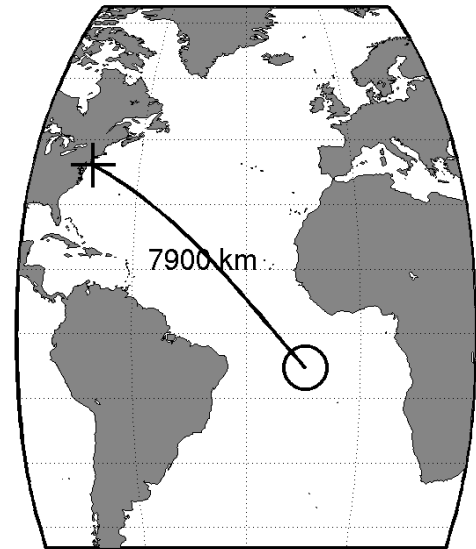


Fig 3. Map showing propagation path between explosion site (cross) and Ascension Island (circle).

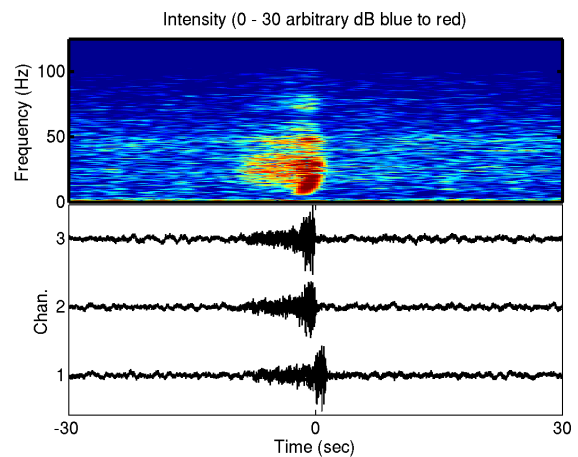


Fig 4. Signals measured on northern triad. Upper pane shows single signal spectrogram. Lower pane shows time histories of all three signals.

The peak arrival times of the signals on the number 2 and 3 hydrophones are approximately the same, while the peak arrival at the number one hydrophone occurs over a second later. This structure, when combined with the locations of the hydrophones (Fig. 1) indicates that the signal arrived from the northwest. To calculate the precise back-azimuth of the arrival, the three waveforms were correlated using a multi-channel technique [PMCC]. This allows signal association to be confirmed on the basis of the peak correlation. Time lags corresponding to the peak correlations can be combined with hydrophone latitudes and longitudes to give the back-azimuth of the arrival.

The explosion location shown in Fig. 2 indicates that it occurred in water of depth less than 100 m. In order for sound transmitted in such shallow water to couple into the deep sound channel, the most likely path is via grazing

reflection at a down-sloping seabed, a process that has been identified [Urlick] as causing ambient noise at a deep hydrophone in Bermuda to be dominated by shipping noise from the continental shelf area in which the explosion occurred. The presence of an initial, shallow water element to the propagation path is the probable reason for the absence of signal energy at frequencies below 5Hz. At such low frequencies, the shallow water column would not act as a waveguide to support propagation during the approximately 50-km journey from explosion site to shelf edge.

3 Predicted and observed arrival properties

The signals received at Ascension Island were observed to have arrival times and azimuths given in Table 1, which also shows the travel times predicted from tables and combines these with the known event time to give a predicted arrival time. Triads are treated as single measuring devices yielding azimuth and a time averaged over the three hydrophones. Also shown in the table are the predicted arrival times and azimuths for the two other IMS hydroacoustic stations that were in operation at the time of the explosion and which had possible paths to the explosion site but which showed no detection.

Stat.	Travel Time (h:m:s)	Arr. Time (UTC)		Arr. Az. (deg)	
		Pred.	Obs.	Pred.	Obs.
H10N	1:29:15	00:34:11	00:34:13	315.5	315.7
H10S	1:30:08	00:35:05	00:35:04	315.9	315.7
H07S	0:40:01	23:44:57*	-	283.2	-
H01W	3:54:00	02:58:56	-	231.1	-

Table 1. Predicted travel times, along with predicted and observed arrival times and azimuths, for signals at four IMS stations. Asterisk indicates arrival on 2nd of August, all other arrivals times on the 3rd of August.

Table 1 shows close agreement between observed and predicted travel times. Differences of around one second correspond to less than the time taken for the signal to traverse the triad and can be considered vanishingly small. To put the remaining disagreement into context, if travel time were estimated by the simplest approach [UAM2009] of dividing the great-circle distance between source and receiver by a deep-water average sound speed of 1485 ms⁻¹ then the predicted arrival time would be around thirty seconds away from the observed value. Although thirty seconds would represent a very small proportion (0.5%) of the total travel time, the ability of travel time tables to reduce the mismatch even further is demonstrated by the data in Table 1.

The signal time histories shown in Fig. 3 indicate that the signal duration was of the order of 10 seconds, significantly longer than the disagreement between observed and predicted arrival times. This emphasizes the importance of the use of full-field modeling techniques in the calculation of travel times [UAM2009]. The travel time tables contain values derived after synthesized signal time histories were input to an algorithm that calculated a probability-weighted arrival time, t_{pw} , [Hanson et al] which represents a best estimate of the peak energy arrival time. The calculation of t_{pw} involves a weighted sum of the times of all samples within the duration of the signal, with the weight for each sample being the probability that the sample is the peak energy arrival time. The probability is calculated taking into account the sample intensity, maximum observed sample intensity and the signal SNR. This algorithm takes account of the multi-peak nature of underwater acoustic signals that results from multipath propagation and coherent interference. Since the same algorithm is used in both the calculation of the travel time tables and the calculation of the arrival time of the measured signals, mismatch between observed and measured arrival times is minimized.

The observed and predicted azimuth values in Table 1 also show very small mismatches. To determine the significance of the azimuth mismatch, it is first necessary to estimate the accuracy to which the azimuth can be measured by the method of calculating time delays at hydrophone triads. This process is subject to errors arising from timing uncertainty and imperfect knowledge of the locations of the hydrophones. Positional imprecision can stem from uncertainty in the location of the seafloor mooring from which the hydrophones are floated and from possible lateral motion of the hydrophone buoys due to ocean currents.

The automatic processing at CTBTO estimates the azimuth uncertainty by correlating signals in a series of separate combinations of time windows and frequency bands. The uncertainty of the azimuth calculation is taken from the variance of these independent estimates. While this is a robust method of uncertainty calculation, it is likely to over-estimate uncertainty because the timing accuracy is reduced by the use of smaller bandwidths. The incoherent average of sub-band uncertainties will be greater than the uncertainty achievable from a full-band calculation by a factor of the order of the square root of the number of sub-bands.

An upper limit on the azimuth uncertainty achievable over the full band can be obtained by consideration of the fundamental process by which azimuth is estimated at triads and this is now performed.

The angle subtended by a wavefront with the line joining a pair of hydrophones can be estimated by correlating the signals to determine the time delay, d , between the arrival of the wave at the two sensors. The expression

$$cd = L \sin \theta \quad (1)$$

relates delay, d , to the local sound speed, c , the separation of the hydrophones, L and the angle θ . Simple differentiation of this equation relates the uncertainty in delay measurement to that in angle expression

$$\delta_{\theta} = \frac{c}{L \cos \theta} \delta_d \quad (2)$$

This shows that uncertainty increases as angle increases. For the triad arrangement, the maximum value of this expression over all three hydrophone pairs will occur for an angle of incidence of 30 degrees since any further increase of angle at one hydrophone pair will correspond to a decrease at another pair.

Signals with sufficiently high signal-to-noise ratio (SNR) have an uncertainty in the delay, d , that is equal to one over the signal bandwidth. The signals shown in Fig. 4 have high SNR (around 20 dB) so this assumption seems reasonable. The spectrogram in the figure indicates that their bandwidth is approximately 50Hz. Substitution of this into Eq. (2), along with a separation of 2000 m, an estimated sound speed of 1485 ms^{-1} and an angle of 30 degrees gives an estimate of the maximum azimuth uncertainty of the order of 1° .

This estimate is for the uncertainty of a measurement at the best-oriented hydrophone pair and takes no account of the extra information that might be derived from the two remaining pairs. This is consistent with the attempt to produce an upper limit on the uncertainty. The estimate does not account for uncertainty in hydrophone positions. This uncertainty is estimated to be of the order of 10m [SashaIce] and such distances cannot be resolved to the accuracy supported by the 50-Hz-bandwidth signals arising from the explosion under consideration here. The effects of positional uncertainty for this application are therefore considered to be negligible.

Uncertainty estimates for broadband, ice-breaking signals arriving on IMS hydrophone triads have been made [SashaIce] using a more rigorous approach including the effect of hydrophone positional uncertainty. This approach used an assumption rms positional uncertainty of 10m and yielded an estimate of azimuthal uncertainty of 0.5° which is broadly in agreement with the upper limit estimated here. The lower value for the ice-breaking signals is consistent with the fact that they are observed to have high SNR over the entire 100 Hz band of the recorded signals.

The azimuthal uncertainty in the arrival information is therefore larger than the mismatch between observed and predicted azimuths. This means that the observed and predicted azimuths are effectively equal and there is no evidence of the effects of out-of-plane refraction or reflection of sound during propagation from explosion site to receivers.

The absence of out-of plane effects is perhaps surprising, considering that bottom reflection is the most likely mechanism by which sound coupled from the shallow water explosion site to the receivers in the deep sound channel. Such a reflection might be expected to include an out-of-plane component that would cause the propagation

path from explosion to receiver to deviate from the route assumed in the prediction of arrival azimuth. The shelf edge close to the explosion site covers an increase in depth of approximately 2000 m over a distance of 25 km, equivalent to an average angle of around 4.5 degrees – relatively large for a seabed slope. However, the great circle route from the explosion site to the receiver locations, shown in Fig. 2, is oriented close to the line of steepest descent down the slope and this fortuitous arrangement is likely to have reduced out-of-plane effects below an observable level.

4 Stations missing detections

Possible paths exist to two other stations in the IMS hydroacoustic network but no signal was observed at these stations and the reasons for these absences are now discussed.

The first such station is H07 which has seismometer sensors installed on the Islands of Flores and Corvo in the Azores. Near-coast seismometers are used in five of the eleven stations that make up the IMS hydroacoustic network. They are intended to detect in-water sound when that sound couples into seismic waves as it travels towards the coast. Seismometers in such locations often detect waterborne signals from distant earthquakes: the so-called tertiary or T-phase [IASPEI]. For this reason seismometer stations are often referred to as “T-phase stations” although this name is misleading since they are not only intended to detect T-phase signals and are part of the IMS network because of their potential capability to detect signals from in-water explosions: so-called H-phases [IASPEI]. For this reason, the nomenclature “T-stations” is preferred.

T-stations suffer from increased levels of background noise due to wave-breaking activity on the nearby shore. Their ability to detect in-water sound is also limited by the high intensity losses associated with seismo-acoustic transmission across the seabed and through the coast. Further difficulties occur because coupling from water waves to crustal waves will not occur in a single process and it is likely that surface, compressional and transverse waves will be generated at different seabed locations. The energy arriving at the seismometer will consequently be spread out over a period significantly longer than the duration of the in-water signal.

These factors mean that the absence of any detection of the signal at the H07 seismometers is easily explicable in terms of SNR considerations.

The H01W hydrophone triad is located 360 km SSW of Perth in Western Australia, more than 21,000 km away from the explosion site. While it might seem impossible that a small explosion should be heard on the opposite side of the world, the signal properties at H10N, combined with a simple detection calculation, suggest that detection was a possibility.

Propagation from the explosion to H10N and H01W was assumed to be described by cylindrical spreading of

energy, with a range-linear reduction in intensity due to temporal dispersion (pulse spreading) and an energy absorption whose band-averaged value is taken [Urick] to be 0.003 dB/km. Under this model, 8.5dB extra propagation loss should be applied when comparing signal intensity at H10N and H01W. The average noise level at H01W was observed to be 9dB higher than that at H10N and this suggested that the SNR of the signals received at H01W should have been (8.5+9=) 17.5 dB below that at H10N. Since the signals in Fig. 4 had a peak intensity approximately 20 dB above the noise level, this suggested that the peak-intensity SNR at H01W should have been about +2.5dB. If this had been precisely the case, then the signal should have been detected. However, the propagation loss prediction used here is subject to considerable uncertainty and detection is best described as being predicted to be marginal. However, the absence of detections at H01W cannot be explained by SNR considerations alone.

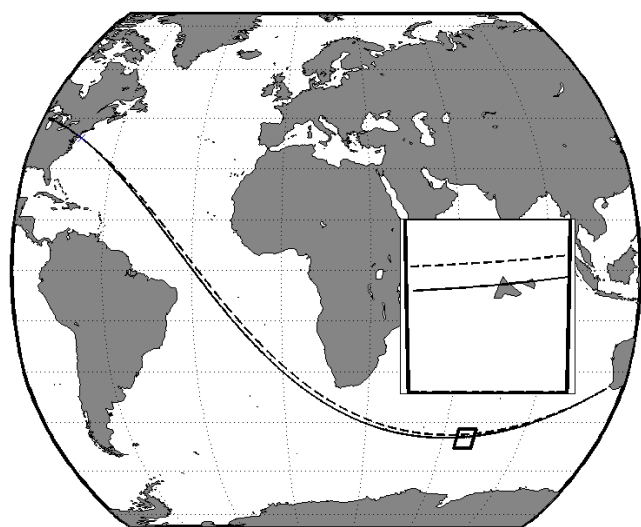


Fig 5. Paths from explosion site to H01W calculated using a spherical earth model (solid line) and the 1980 Geodetic Reference System ellipsoid (dashed line). Inset shows detail around the Kerguelen Islands.

The dashed line in Fig. 5 shows the explosion-receiver path calculated using the 1980 Geodetic Reference System ellipsoid [Moritz] for the Earth. A solid line representing the great-circle path between the two locations is also shown in the figure. The inset shows the detail of the two paths in the vicinity of the Kerguelen Islands and the ellipsoidal path is shown to pass around 100km to the north of the islands while the great circle route is blocked by them.

The ellipsoidal path avoids blockage by the Kerguelen Islands but it crosses a shallow water area where deep-sound channel propagation is interrupted. The only way that sound could cross this region is by repeated interaction with the seabed and the extra energy losses associated with this would undoubtedly attenuate the signal.

Out-of-plane reflection at the seabed and horizontal refraction due to mesoscale ocean features and internal

waves can deflect the paths taken by sound away from those shown in Fig. 5. Signals have been received near Bermuda [Heaney, Dushaw, Munk] from an explosion site near Perth when the receiver was nominally in the shadow cast by the Cape of Good Hope. However, these effects tend to be small and likely to be insufficient to divert sound away from the shallow-water region around the Kerguelen Islands, which extends for many hundreds of kilometers offshore.

Thus, the most probable explanation for the absence of detections at H01W is the “effective blockage” of the acoustic path by the shallow water around the Kerguelen Islands.

5 Summary and discussion

Signals resulting from the accidental explosion on the New Jersey Shelf were received nearly 8000 kilometres away at the IMS hydrophone stations at Ascension Island.

The observed arrival times were shown to be within 2 seconds of those predicted using ground-truth knowledge of the explosion’s time and location, combined with look-up tables of travel time to the stations. The agreement between predicted and observed arrival times was less than the time taken for the sound to transit the area covered by the receiving hydrophones and significantly less than the signal duration which was around 10 seconds.

The difference between observed arrival azimuth and values predicted while neglecting out-of-plane reflection and refraction processes was shown to be less than the estimated measurement uncertainty. This uncertainty was estimated to be about 1° for the 50-Hz bandwidth signals.

The good agreement described above provides a striking demonstration of the capabilities of the network of sensors operated by CTBTO. The ability to relate arrival time and generating-event time to accuracies of the order of seconds allows the network to locate underwater explosions precisely.

Time and azimuth information of this kind is routinely combined with similar information from other sensors at CTBTO. These sensors cover three waveform types: hydroacoustic, seismic and infrasound. Final event location is determined by numerical minimization of weighted time- and azimuth residuals where a “residual” is the difference between the observed arrival time and the arrival time that would be associated with a hypothesized event time and location. The weightings used in this minimization process are estimates of the accuracy associated with the various measurements. Arrival time uncertainty varies considerably between waveform types and accurate estimates of this uncertainty are vital if good event locations are to be formed.

The seismic network of the IMS detects signals from many earthquakes every day. Many of these earthquakes are independently located by local seismic networks which,

while not providing the global coverage of the IMS, are more accurate in their limit region of applicability. Thus, estimates of uncertainty in arrival time and azimuth from the seismic network can be made using these independent, local solutions.

The infrasound network of the IMS detects signals from man-made events such as mining blasts and launches of spacecraft like the NASA Space Shuttle [Infrashuttle]. The times and places of these events can be ascertained independently and time and azimuth uncertainties can be estimated.

Such ground-truth data is less easily obtained for the hydroacoustic network. Underwater explosions are regularly detected on the network from sources such as military exercises or illegal blast-fishing [HansonBlast] but it is not usually possible to obtain event times and locations for these.

The detection of signals from the accidental explosion described here therefore represents a rare and valuable opportunity to assess IMS hydroacoustic network measurement accuracy to improve the event-locating capability of the entire IMS network.

References

- [1] deGroot-Hedlin, C., and Orcutt, J. (Eds), "Monitoring the Comprehensive Nuclear-Test-Ban Treaty: Hydroacoustics," *Pure and Applied Geophysics*, 158(3), pp. 421-626, 2001.
- [2] Urick, R. J. *Principles of Underwater Sound; 3rd edition*. (McGraw-Hill), 1983.
- [3] Hanson, J., Le Bras, R., Dysart, P., Brumbaugh, D. and Gault, A., "Operational processing of hydroacoustic data at the Prototype International Data Center", *Pure and Applied Geophysics* 158(3), pp. 425-456, 2001.
- [4] Husebye E.S. and Dainty A. M. (Eds), *Monitoring a Comprehensive Test-Ban Treaty* (Kluwer), 1996.
- [5] Prior, M. K. "Improving the accuracy of in-water travel-time predictions for seismic event location using two-dimensional underwater acoustic propagation modelling", In *Underwater Acoustic Measurements, Technologies and Results: 3rd International Conference and Exhibition, Nafplion, Greece*. (Available from site location <http://www.uam2009.gr/proceedings.php>, last viewed 26/04/2010), 2009.
- [6] Cansi Y., "An automatic seismic event processing for detection and location: The P.M.C.C. method, *Geophys. Res. Lett.*, 22, 1021-1024, 1995.
- [7] Li, B. And Gavrilov, A. N. "Hydroacoustic observation of Antarctic ice disintegration events in the Indian Ocean." In *Proceedings of ACOUSTICS 2006, Christchurch, New Zealand*. pp 479-484. 2006
- [8] Hanson, J. A., Reasoner, C. L. and Bowman, J. R., "Hydroacoustic propagation and reflection loss using explosions found in the Indian Ocean", 29th Seismic Research Symposium. 2007. (available from site location <http://www.rdss.info>, last viewed 02/13/09)